

## Supporting information

### Machine learning for tailoring optoelectronic properties of single-walled carbon nanotube films

Eldar M. Khabushev<sup>1</sup>, Dmitry V. Krasnikov<sup>\*,1</sup>, Orysia T. Zaremba<sup>1</sup>, Alexey P. Tsapenko<sup>1,2</sup>, Anastasia E. Goldt<sup>1</sup>, and Albert G. Nasibulin<sup>\*,1,2</sup>

<sup>1</sup> Skolkovo Institute of Science and Technology, Nobel street 3, 121205 Moscow, Russian Federation

<sup>2</sup> Aalto University, PO. 16100, 00076 Espoo, Finland

#### Materials and methods

Single-walled carbon nanotube (SWCNT) films were synthesized using a laboratory-scale tubular quartz reactor (with an inner diameter of 7.25 cm, length of 150 cm, including 70 cm of the isothermal zone with temperature regulated to within 1°C) operating at atmospheric pressure. Ferrocene was used as a catalyst precursor: a CO flow (>99.995%) was passed through a cartridge with a ferrocene/silica mixture, introducing a precursor vapor (0.9 Pa at a fixed temperature of 24 °C)<sup>1</sup> in the reactor isothermal zone through an injector. A volumetric fraction of ferrocene (catalyst precursor) inside the reactor was tuned in the range of 0.15–1.20 ppm, adjusting CO flow rate through the cartridge. Another flow consisted of a CO/CO<sub>2</sub> mixture was introduced from the main inlet; total volumetric fraction of CO<sub>2</sub> was varied in the range from 0 to 2.2 vol. % with an accuracy of almost 0.01 vol. % limited by the precision of mass flow meter used. The total flow rate through the reactor was fixed at 5000 standard cm<sup>3</sup>/min. The aerosol containing carbon nanotubes was deposited by a simple filtration at the outlet of the reactor using 13 mm-sized nitrocellulose membrane filter (MF-Millipore, 0.45 μm pore size) placed in Milipore Swinny Filter Holder. SWCNTs

formed a round uniform film with the diameter of 11 mm. For characterization all collected films were transferred onto a glass by the dry deposition technique.<sup>2</sup>

The transmittance of the films as well as the yield of SWCNTs was obtained from optical absorption spectroscopy performed in the wavelength range from 250 to 2600 nm with 1 nm step using Perkin Elmer UV-vis-NIR spectrophotometer Lambda 1050. Morphology of the samples was observed by FEI Tecnai G2 F20 transmission electron microscope (TEM). For TEM observations, SWCNTs were directly collected on TEM-grids (PELCO Carbon 400 Mesh Cu, 42  $\mu\text{m}$  hole size, TED PELLA Inc.) via putting it directly within the aerosol stream.

The sheet resistance of the films was measured by four-probe station Jandel RM3000, which served both as the current supply and a voltmeter. The measurements for each film were repeated at least three times (in different directions) and obtained values were averaged. The current was varied from 0.01 to 1 mA depending on a sample conductivity. The reproducibility of sheet resistance values (at certain synthesis conditions) from sample to sample was estimated to be relatively high: a relative standard deviation value was close to 4% (Table S2). Doping of the films was carried out using Xdip-MV1 Apex Instruments dip-coating system by immersing films into 15 mM ethanol solution of  $\text{HAuCl}_4$  (99.9% Acros) at 100 mm/min speed. The films were remained inside solution for 20 seconds and pulled up at constant speed of 100 mm/min.

### **Optimal ferrocene concentration**

We enhance the results obtained by reducing the SWCNT agglomeration degree (Figure S1), which significantly affects<sup>3</sup> the SWCNT film performance. The formation of the agglomerates is mostly attributed to the Brownian motion of nanotubes within the aerosol, which is slightly affected by the temperature (with an activation energy of  $\sim RT$ )<sup>4</sup> and not affected by  $\text{CO}_2$  concentration at all. Here we also consider the effect of  $\text{CO}_2$  and the growth temperature negligible on ferrocene decomposition itself, as the decomposition starts at  $T > 400^\circ\text{C}$ <sup>5</sup> so the 800-1050  $^\circ\text{C}$  region is significantly warmer and decomposition itself occurs before the isothermic zone. Thus, with the SWCNT defectiveness and purity being optimized by

the growth temperature and CO<sub>2</sub> fraction, we independently adjust the concentration of the catalyst precursor to control the agglomeration degree of nanotubes. When studying the influence of the ferrocene concentration, we observed an optimum in a specific yield (in catalyst mass) at  $C_{\text{Fe}(\text{Cp})_2} = 0.6$  ppm (Figure S1a).

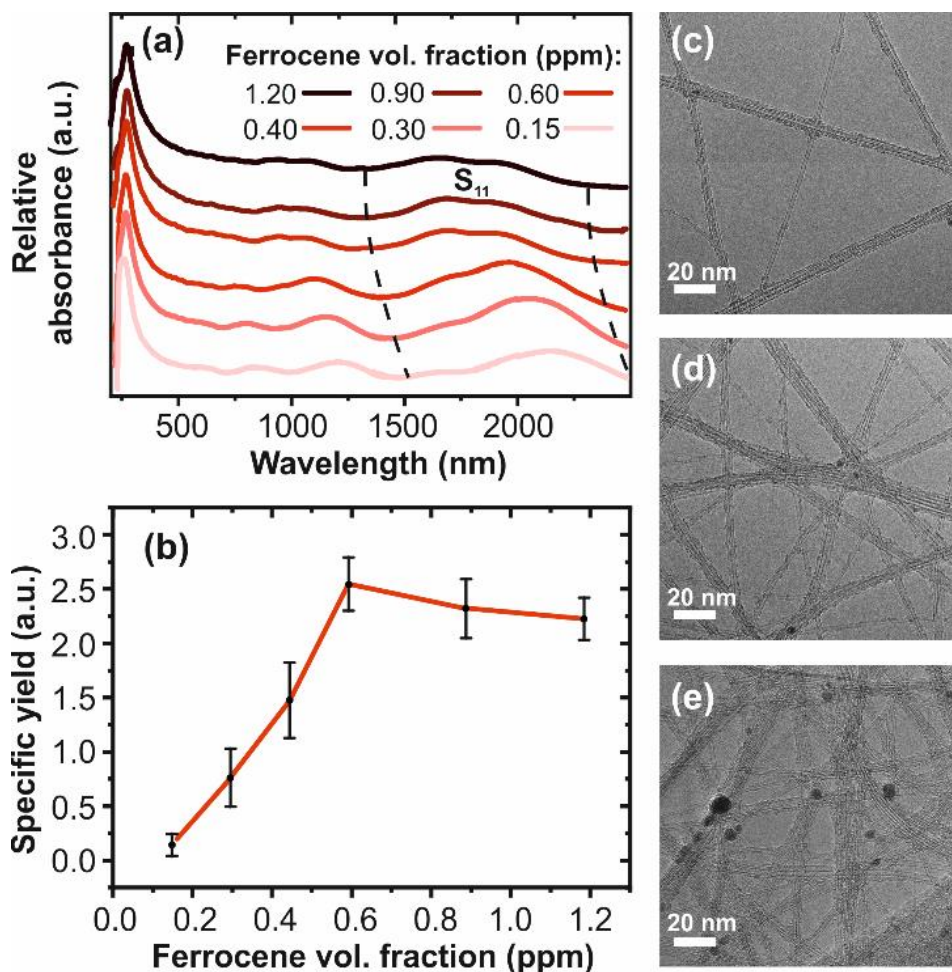


**Figure S1.** (a) Optical spectra of the films produced at 850°C and  $x_{\text{CO}_2} = 0.6\%$ . (b) The influence of the ferrocene concentration on the specific yield of SWCNTs (estimated from the absorbance at 550 nm) representing catalyst productivity with the highest value at  $C_{\text{Fe}(\text{Cp})_2} = 0.6$  ppm. (c), (d), (e) Representative TEM images of SWCNTs collected at 0.3, 0.6, and 1.2 ppm of ferrocene, correspondingly.

The TEM studies (Figure S1c-e) prove an increase in the purity of carbon nanotubes with a lower concentration of the precursor. Moreover, the ferrocene concentration lower than 0.6 ppm increases the mean diameter of SWCNTs obtained (Figure S1a) breaking, thereby, the SVR-based optimization. Thus, we

choose the 0.6 ppm precursor concentration to be the optimal one (the highest specific yield, no change in SWCNT characteristics).

### Reproducibility of the data

To illustrate the reproducibility of equivalent sheet resistance, we characterized 5 samples collected at certain reaction conditions ( $T=900\text{ }^{\circ}\text{C}$ ,  $x_{\text{CO}_2}=1.1\text{ vol. \%}$ ). The  $R_{90}$  data, presented in Table S, has a relative standard deviation of 4%.

Table S1. Transparent and conductive properties of the films collected at  $900\text{ }^{\circ}\text{C}$  and  $1.1\text{ vol. \%}$  of  $\text{CO}_2$  ( $A_{550}$  – SWCNT film absorbance at the wavelength of  $550\text{ nm}$ ;  $R_s$  – sheet resistance).

Sample №	$A_{550}$	$R_s, \Omega/\square$			$M.R_s, \Omega/\square$	$R_{90}, \Omega/\square$
1	0.268	289	278	298	288	1692
2	0.250	297	294	274	288	1580
3	0.288	247	250	260	252	1591
4	0.264	275	268	276	273	1577
5	0.262	285	285	270	280	1605

### References

- (1) Fulem, M.; Růžicka, K.; Červinka, C.; Rocha, M. A. A.; Santos, L. M. N. B. F.; Berg, R. F. Recommended Vapor Pressure and Thermophysical Data for Ferrocene. *J. Chem. Thermodyn.* **2013**, *57*, 530–540.
- (2) Kaskela, A.; Nasibulin, A. G.; Timmermans, M. Y.; Aitchison, B.; Papadimitratos, A.; Tian, Y.; Zhu, Z.; Jiang, H.; Brown, D. P.; Zakhidov, A.; et al. Aerosol-Synthesized SWCNT Networks with Tunable Conductivity and Transparency by a Dry Transfer Technique. *Nano Lett.* **2010**, *10*, 4349–4355.
- (3) Mustonen, K.; Laiho, P.; Kaskela, A.; Zhu, Z.; Reynaud, O.; Houbenov, N.; Tian, Y.; Susi, T.; Jiang, H.; Nasibulin, A. G.; et al. Gas Phase Synthesis of Non-Bundled, Small Diameter Single-Walled Carbon Nanotubes with near-Armchair Chiralities. *Appl. Phys. Lett.* **2015**, *107*, 10–15.

- (4) Hinds, W. C. *Aerosol Technology*, 2nd ed.; Wiley, New York, 1999.
- (5) Kuwana, K.; Saito, K. Modeling CVD Synthesis of Carbon Nanotubes: Nanoparticle Formation from Ferrocene. *Carbon* **2005**, *43*, 2088–2095.